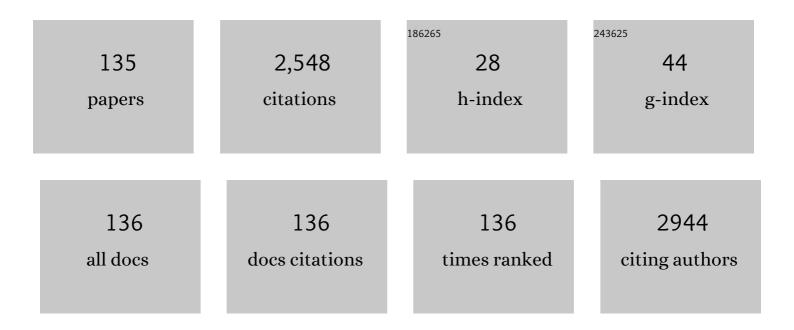
List of Publications by Year in descending order

Source: https://exaly.com/author-pdf/4077497/publications.pdf Version: 2024-02-01



#	Article	IF	CITATIONS
1	Charge trapping processes in hydrothermally grown Er-doped ZnO. Radiation Measurements, 2022, 150, 106700.	1.4	7
2	Hydrothermally grown ZnO:Mo nanorods exposed to X-ray: Luminescence and charge trapping phenomena. Applied Surface Science, 2022, 585, 152682.	6.1	11
3	Plasma Treatment of Gaâ€Doped ZnO Nanorods. Physica Status Solidi (A) Applications and Materials Science, 2022, 219, .	1.8	1
4	Free-Standing ZnO:Mo Nanorods Exposed to Hydrogen or Oxygen Plasma: Influence on the Intrinsic and Extrinsic Defect States. Materials, 2022, 15, 2261.	2.9	7
5	Nanodiamond surface chemistry controls assembly of polypyrrole and generation of photovoltage. Scientific Reports, 2021, 11, 590.	3.3	10
6	Microscopic Study of Bovine Serum Albumin Adsorption on Zinc Oxide (0001) Surface. Physica Status Solidi (A) Applications and Materials Science, 2021, 218, 2170024.	1.8	0
7	Enhanced Photodegradation in Metal Oxide Nanowires with Co-Doped Surfaces under a Low Magnetic Field. ACS Applied Materials & amp; Interfaces, 2021, 13, 23173-23180.	8.0	10
8	Growth Inhibition of Gram-Positive and Gram-Negative Bacteria by Zinc Oxide Hedgehog Particles. International Journal of Nanomedicine, 2021, Volume 16, 3541-3554.	6.7	20
9	Single-Source Pulsed Laser Deposition of MAPbI3. , 2021, , .		1
10	Pulsed laser deposition of high-transparency molybdenum oxide thin films. Vacuum, 2021, 194, 110613.	3.5	4
11	Microscopic Study of Bovine Serum Albumin Adsorption on Zinc Oxide (0001) Surface. Physica Status Solidi (A) Applications and Materials Science, 2021, 218, 2000558.	1.8	4
12	Emergence of DARK ZnO Nanorods by Hydrogen Plasma Treatment. , 2021, , .		0
13	Transformation of ZnO-based structures under heavy Mo doping: defect states and luminescence. , 2021, , .		2
14	Plasma-synthesised Zinc oxide nanoparticle behavior in liquids. , 2021, , .		0
15	Optical characterization of low temperature amorphous MoOx, WOX, and VOx prepared by pulsed laser deposition. Thin Solid Films, 2020, 693, 137690.	1.8	11
16	Manipulated Optical Absorption and Accompanied Photocurrent Using Magnetic Field in Charger Transfer Engineered C/ZnO Nanowires. Global Challenges, 2020, 4, 2000025.	3.6	1
17	Singleâ€Source, Solventâ€Free, Room Temperature Deposition of Black γ sSnI ₃ Films. Advanced Materials Interfaces, 2020, 7, 2000162.	3.7	32
18	Highâ€Temperature PIN Diodes Based on Amorphous Hydrogenated Siliconâ€Carbon Alloys and Boronâ€Doped Diamond Thin Films. Physica Status Solidi (B): Basic Research, 2020, 257, 1900247.	1.5	4

#	Article	IF	CITATIONS
19	Room temperature plasma hydrogenation – An effective way to suppress defects in ZnO nanorods. Materials Today: Proceedings, 2020, 33, 2481-2483.	1.8	8
20	plasma HYDROGENATION OF HYDROTHERMALLY GROWN ZnO MICROPODS. , 2020, , .		2
21	Optoelectronic Properties of Hydrogenated Amorphous Substoichiometric Silicon Carbide with Low Carbon Content Deposited on Semiâ€Transparent Boronâ€Doped Diamond. Physica Status Solidi (A) Applications and Materials Science, 2019, 216, 1900241.	1.8	5
22	Electrical and optical characteristics of boron doped nanocrystalline diamond films. Vacuum, 2019, 168, 108813.	3.5	8
23	Manipulation of the magnetoabsorption effect in Co-coated ZnO nanowires with Au decoration. Applied Surface Science, 2019, 492, 591-597.	6.1	3
24	Maximized vertical photoluminescence from optical material with losses employing resonant excitation and extraction of photonic crystal modes. Nanophotonics, 2019, 8, 1041-1050.	6.0	5
25	Synthesis and properties of diamond - silicon carbide composite layers. Journal of Alloys and Compounds, 2019, 800, 327-333.	5.5	9
26	Ytterbium silicide nanostructures prepared by pulsed laser ablation in oven: Structural and electrical characterization. Materials Letters, 2019, 246, 17-19.	2.6	0
27	Effect of a-Si on CH3NH3PbI3 Films and Applications in Perovskite Solar Cells. , 2019, , .		0
28	Electroluminescence of thin film <i>p-i-n</i> diodes based on a-SiC:H with integrated Ge nanoparticles. EPJ Applied Physics, 2019, 88, 30302.	0.7	5
29	Study of ZnO nanorods grown under UV irradiation. Applied Surface Science, 2019, 472, 105-111.	6.1	41
30	Nanocrystalline diamond films heavily doped by boron: structure, optical and electrical properties. , 2019, , .		0
31	Coâ€implantation of Er and Yb ions into singleâ€crystalline and nanoâ€crystalline diamond. Surface and Interface Analysis, 2018, 50, 1218-1223.	1.8	7
32	Raman scattering in boron doped nanocrystalline diamond films: Manifestation of Fano interference and phonon confinement effect. Solid State Communications, 2018, 276, 33-36.	1.9	11
33	Precursor gas composition optimisation for large area boron doped nano-crystalline diamond growth by MW-LA-PECVD. Carbon, 2018, 128, 164-171.	10.3	26
34	Thermal sulfidation of α-Fe2O3 hematite to FeS2 pyrite thin electrodes: Correlation between surface morphology and photoelectrochemical functionality. Catalysis Today, 2018, 313, 224-230.	4.4	12
35	Synthesis of zinc oxide nanostructures and comparison of their crystal quality. Applied Surface Science, 2018, 461, 190-195.	6.1	29
36	Refractive indices of layers and optical simulations of Cu(In,Ga)Se ₂ solar cells. Science and Technology of Advanced Materials, 2018, 19, 396-410.	6.1	46

#	Article	IF	CITATIONS
37	Erbium Luminescence Centres in Single- and Nano-Crystalline Diamond—Effects of Ion Implantation Fluence and Thermal Annealing. Micromachines, 2018, 9, 316.	2.9	5
38	Measurement of doping profiles by a contactless method of IR reflectance under grazing incidence. Review of Scientific Instruments, 2018, 89, 063114.	1.3	0
39	Erbium ion implantation into diamond – measurement and modelling of the crystal structure. Physical Chemistry Chemical Physics, 2017, 19, 6233-6245.	2.8	18
40	Photocurrent Spectroscopy of Perovskite Layers and Solar Cells: A Sensitive Probe of Material Degradation. Journal of Physical Chemistry Letters, 2017, 8, 838-843.	4.6	18
41	Optically transparent composite diamond/Ti electrodes. Carbon, 2017, 119, 179-189.	10.3	18
42	Nickel oxide films by thermal annealing of ion-beam-sputtered Ni: Structure and electro-optical properties. Thin Solid Films, 2017, 640, 52-59.	1.8	4
43	Formation and study of p–i–n structures based on two-phase hydrogenated silicon with a germanium layer in the i-type region. Semiconductors, 2017, 51, 1370-1376.	0.5	6
44	Enhancing the optoelectronic properties of amorphous zinc tin oxide by subgap defect passivation: A theoretical and experimental demonstration. Physical Review B, 2017, 95, .	3.2	31
45	Optical properties of the plasma hydrogenated ZnO thin films. Journal of Electrical Engineering, 2017, 68, 70-73.	0.7	6
46	Production of zinc oxide nanowires power with precisely defined morphology. Journal of Electrical Engineering, 2017, 68, 66-69.	0.7	0
47	Study of the surface properties of ZnO nanocolumns used for thin-film solar cells. Beilstein Journal of Nanotechnology, 2017, 8, 446-451.	2.8	22
48	Preparation and optical properties of nanocrystalline diamond coatings for infrared planar waveguides. Thin Solid Films, 2016, 618, 130-133.	1.8	23
49	Optical properties of p–i–n structures based on amorphous hydrogenated silicon with silicon nanocrystals formed via nanosecond laser annealing. Semiconductors, 2016, 50, 935-940.	0.5	10
50	Structural, optical and mechanical properties of thin diamond and silicon carbide layers grown by low pressure microwave linear antenna plasma enhanced chemical vapour deposition. Diamond and Related Materials, 2016, 69, 13-18.	3.9	20
51	Fabrication of diamond-coated germanium ATR prisms for IR-spectroscopy. Vibrational Spectroscopy, 2016, 84, 67-73.	2.2	3
52	Effect of plasma composition on nanocrystalline diamond layers deposited by a microwave linear antenna plasmaâ€enhanced chemical vapour deposition system. Physica Status Solidi (A) Applications and Materials Science, 2015, 212, 2418-2423.	1.8	15
53	Nâ€Vâ€related fluorescence of the monoenergetic highâ€energy electronâ€irradiated diamond nanoparticles. Physica Status Solidi (A) Applications and Materials Science, 2015, 212, 2519-2524.	1.8	9
54	Properties of boron-doped epitaxial diamond layers grown on (110) oriented single crystal substrates. Diamond and Related Materials, 2015, 53, 29-34.	3.9	29

#	Article	IF	CITATIONS
55	Ferromagnetism appears in nitrogen implanted nanocrystalline diamond films. Journal of Magnetism and Magnetic Materials, 2015, 394, 477-480.	2.3	11
56	On the improvement of PEC activity of hematite thin films deposited by high-power pulsed magnetron sputtering method. Applied Catalysis B: Environmental, 2015, 165, 344-350.	20.2	41
57	INFRARED PHOTOLUMINESCENCE SPECTRA OF PBS NANOPARTICLES PREPARED BY LANGMUIR–BLODGETT AND LASER ABLATION METHODS. Acta Polytechnica, 2014, 54, 426-429.	0.6	4
58	Siâ€related color centers in nanocrystalline diamond thin films. Physica Status Solidi (B): Basic Research, 2014, 251, 2603-2606.	1.5	6
59	Multiple kinds of emission modes in semiconductor microcavity coupled with plasmon. Physica B: Condensed Matter, 2014, 434, 74-77.	2.7	2
60	High-power pulsed plasma deposition of hematite photoanode for PEC water splitting. Catalysis Today, 2014, 230, 8-14.	4.4	32
61	BaWO <inf>4</inf> intracavity pumped eye-safe Raman laser. , 2014, , .		0
62	Organic–Inorganic Halide Perovskites: Perspectives for Silicon-Based Tandem Solar Cells. IEEE Journal of Photovoltaics, 2014, 4, 1545-1551.	2.5	123
63	Nanostructured Diamond Layers Enhance the Infrared Spectroscopy of Biomolecules. Langmuir, 2014, 30, 2054-2060.	3.5	11
64	Epoxy catalyzed sol–gel method for pinhole-free pyrite FeS2 thin films. Journal of Alloys and Compounds, 2014, 607, 169-176.	5.5	13
65	Surface and Ultrathin-layer Absorptance Spectroscopy for Solar Cells. Energy Procedia, 2014, 60, 57-62.	1.8	3
66	Chemical modifications and stability of diamond nanoparticles resolved by infrared spectroscopy and Kelvin force microscopy. Journal of Nanoparticle Research, 2013, 15, 1.	1.9	31
67	Photoluminescence eigenmodes in the ZnO semiconductor microcavity on the Ag/Si substrate. Applied Physics A: Materials Science and Processing, 2013, 112, 821-825.	2.3	1
68	Deposition of hematite Fe2O3 thin film by DC pulsed magnetron and DC pulsed hollow cathode sputtering system. Thin Solid Films, 2013, 549, 184-191.	1.8	31
69	Diamond-coated ATR prism for infrared absorption spectroscopy of surface-modified diamond nanoparticles. Applied Surface Science, 2013, 270, 411-417.	6.1	17
70	Arrays of ZnO nanocolumns for 3-dimensional very thin amorphous and microcrystalline silicon solar cells. Thin Solid Films, 2013, 543, 110-113.	1.8	18
71	Design and investigation of properties of nanocrystalline diamond optical planar waveguides. Optics Express, 2013, 21, 8417.	3.4	22
72	Technological possibilities of Si:H thin film deposition with embedded cubic Mg ₂ Si nanoparticles. Physica Status Solidi C: Current Topics in Solid State Physics, 2013, 10, 1712-1716.	0.8	10

#	Article	IF	CITATIONS
73	Laser profiling of defects in BaWO4crystals. Measurement Science and Technology, 2012, 23, 087001.	2.6	2
74	Optical study of defects in nanoâ€diamond films grown in linear antenna microwave plasma CVD from H ₂ /CH ₄ /CO ₂ gas mixture. Physica Status Solidi (B): Basic Research, 2012, 249, 2635-2639.	1.5	18
75	Exciton diffusion length in some thermocleavable polythiophenes by the surface photovoltage method. Synthetic Metals, 2012, 161, 2727-2731.	3.9	15
76	ZnO hedgehog-like structures for control cell cultivation. Applied Surface Science, 2012, 258, 3485-3489.	6.1	17
77	Exciton diffusion length and concentration of holes in MEH-PPV polymer using the surface voltage and surface photovoltage methods. Chemical Physics Letters, 2012, 552, 49-52.	2.6	12
78	Grazing angle reflectance spectroscopy of organic monolayers on nanocrystalline diamond films. Diamond and Related Materials, 2011, 20, 882-885.	3.9	13
79	Nanostructured three-dimensional thin film silicon solar cells with very high efficiency potential. Applied Physics Letters, 2011, 98, .	3.3	92
80	Optical characterisation of organosilane-modified nanocrystalline diamond films. Chemical Papers, 2011, 65, .	2.2	9
81	Deposition of nanocrystalline diamond films on temperature sensitive substrates for infrared reflectance spectroscopy. Physica Status Solidi (B): Basic Research, 2011, 248, 2736-2739.	1.5	12
82	Double hollow cathode plasma jet-low temperature method for the TiO2â^'N photoresponding films. Electrochimica Acta, 2010, 55, 1548-1556.	5.2	26
83	Control of tin oxide film morphology by addition of hydrocarbons to the chemical vapour deposition process. Thin Solid Films, 2010, 519, 1334-1340.	1.8	13
84	Optical absorption losses in metal layers used in thin film solar cells. Physica Status Solidi (A) Applications and Materials Science, 2010, 207, 2170-2173.	1.8	1
85	Fourier transform photocurrent measurement of thin silicon films on rough, conductive and opaque substrates. Physica Status Solidi (A) Applications and Materials Science, 2010, 207, 578-581.	1.8	9
86	The optical absorption of metal nanoparticles deposited on ZnO films. Physica Status Solidi (A) Applications and Materials Science, 2010, 207, 1722-1725.	1.8	8
87	High optical quality nanocrystalline diamond with reduced non-diamond contamination. Diamond and Related Materials, 2010, 19, 453-456.	3.9	17
88	Comparison Between Chemical and Plasmatic Treatment of Seeding Layer for Patterned Diamond Growth. Materials Research Society Symposia Proceedings, 2009, 1203, 1.	0.1	0
89	Optimization of Solar Cell Performance using Atmospheric Pressure Chemical Vapour Deposition deposited TCOs. ECS Transactions, 2009, 25, 789-796.	0.5	4
90	Optical Monitoring of Nanocrystalline Diamond with Reduced Non-diamond Contamination. Materials Research Society Symposia Proceedings, 2009, 1203, 1.	0.1	0

#	Article	IF	CITATIONS
91	Towards opticalâ€quality nanocrystalline diamond with reduced nonâ€diamond content. Physica Status Solidi (A) Applications and Materials Science, 2009, 206, 2004-2008.	1.8	8
92	Amorphous silicon solar cells made with SnO2:F TCO films deposited by atmospheric pressure CVD. Materials Science and Engineering B: Solid-State Materials for Advanced Technology, 2009, 159-160, 6-9.	3.5	42
93	Atmospheric pressure chemical vapour deposition of F doped SnO2 for optimum performance solar cells. Thin Solid Films, 2009, 517, 3061-3065.	1.8	58
94	Optical properties of SnO2:F films deposited by atmospheric pressure CVD. Thin Solid Films, 2009, 517, 6287-6289.	1.8	74
95	The infrared optical absorption spectra of the functionalized nanocrystalline diamond surface. Diamond and Related Materials, 2009, 18, 772-775.	3.9	14
96	On the reduction of the non-diamond phase in nanocrystalline CVD diamond films. Diamond and Related Materials, 2009, 18, 726-729.	3.9	9
97	Study of the passivation mechanisms of boron doped diamond using the Amplitude Modulated Step Scan Fourier Transform Photocurrent Spectroscopy. Diamond and Related Materials, 2009, 18, 827-830.	3.9	2
98	Optimum performance solar cells using atmospheric pressure chemical vapour deposition deposited TCOs. International Journal of Nanotechnology, 2009, 6, 816.	0.2	9
99	The influence of thermal annealing on the electronic defect states in nanocrystalline CVD diamond films. Physica Status Solidi (A) Applications and Materials Science, 2008, 205, 2158-2162.	1.8	4
100	Formation of Continuous Nanocrystalline Diamond Layers on Glass and Silicon at Low Temperatures. Chemical Vapor Deposition, 2008, 14, 181-186.	1.3	77
101	Comparison of photocurrent spectra measured by FTPS and CPM for amorphous silicon layers and solar cells. Journal of Non-Crystalline Solids, 2008, 354, 2167-2170.	3.1	18
102	Spectral response of amorphous–nano-crystalline silicon thin films. Journal of Non-Crystalline Solids, 2008, 354, 2286-2290.	3.1	24
103	Photocurrent study of electronic defects in nanocrystalline diamond. Diamond and Related Materials, 2008, 17, 1311-1315.	3.9	8
104	Substrate temperature changes during molecular beam epitaxy growth of GaMnAs. Journal of Applied Physics, 2007, 102, .	2.5	12
105	The RF plasma surface chemical modification of nanodiamond films grown on glass and silicon at low temperature. Diamond and Related Materials, 2007, 16, 671-674.	3.9	21
106	Investigation of nanocrystalline diamond films grown on silicon and glass at substrate temperature below 400°C. Diamond and Related Materials, 2007, 16, 744-747.	3.9	51
107	Amplitude modulated step scan Fourier transform photocurrent spectroscopy of partly compensated Bâ€doped CVD diamond thin films. Physica Status Solidi (A) Applications and Materials Science, 2007, 204, 2950-2956.	1.8	13
108	Time of flight study of high performance CVD diamond detector devices. Physica Status Solidi (A) Applications and Materials Science, 2007, 204, 3023-3029.	1.8	29

#	Article	IF	CITATIONS
109	Nanocrystalline diamond surface functionalization in radio frequency plasma. Diamond and Related Materials, 2006, 15, 745-748.	3.9	31
110	Spectroscopy of thin nanodiamond layers and membranes. Journal of Non-Crystalline Solids, 2006, 352, 1344-1347.	3.1	6
111	Growth of nanocrystalline diamond films deposited by microwave plasma CVD system at low substrate temperatures. Physica Status Solidi (A) Applications and Materials Science, 2006, 203, 3011-3015.	1.8	45
112	Infrared optical properties of heavily B-doped nanocrystalline diamond films on low alkaline glass substrates. Physica Status Solidi (A) Applications and Materials Science, 2006, 203, 3016-3020.	1.8	2
113	LYRA, a solar UV radiometer on Proba2. Advances in Space Research, 2006, 37, 303-312.	2.6	80
114	Performance of diamond detectors for VUV applications. Nuclear Instruments and Methods in Physics Research, Section A: Accelerators, Spectrometers, Detectors and Associated Equipment, 2006, 568, 398-405.	1.6	31
115	Single Crystal CVD Diamond growth and characterizations. Materials Research Society Symposia Proceedings, 2006, 956, 1.	0.1	1
116	The optical absorption and photoconductivity spectra of hexagonal boron nitride single crystals. Physica Status Solidi A, 2005, 202, 2229-2233.	1.7	40
117	Mechanism of photoconductivity in intrinsic epitaxial CVD diamond studied by photocurrent spectroscopy and photocurrent decay measurements. Diamond and Related Materials, 2005, 14, 556-560.	3.9	35
118	Structural, optical and electrical properties of nanodiamond films deposited by HFCVD on borosilicate glass, fused silica and silicon at low temperature. Physica Status Solidi A, 2004, 201, 2499-2502.	1.7	12
119	Defect-dopant interaction in n- and p-type diamond and its influence on electrical properties. Diamond and Related Materials, 2004, 13, 722-726.	3.9	5
120	Photo-Hall effect measurements in P, N and B-doped diamond at low temperatures. Diamond and Related Materials, 2004, 13, 713-717.	3.9	7
121	Solar-Blind Diamond Detectors for Lyra, the Solar VUV Radiometer on Board Proba II. Experimental Astronomy, 2003, 16, 141-148.	3.7	9
122	Photo-Hall measurements on phosphorus-doped n-type CVD diamond at low temperatures. Physica Status Solidi A, 2003, 199, 82-86.	1.7	4
123	Temperature dependence of intrinsic infrared absorption in natural and chemical-vapor deposited diamond. Journal of Applied Physics, 2002, 92, 756-763.	2.5	13
124	Why Does Diamond Absorb Infra-Red Radiation?. Physica Status Solidi A, 2002, 193, 442-447.	1.7	6
125	Local Variations and Temperature Dependence of Optical Absorption Coefficient in Natural IIa Type and CVD Diamond Optical Windows. Physica Status Solidi A, 2001, 186, 297-301.	1.7	8
126	Photothermal Deflection Mapping of Variations in the Optical Absorption in IR Windows. Physica Status Solidi A, 2000, 181, 115-119.	1.7	2

#	Article	IF	CITATIONS
127	Scanning Tunneling Microscopy and Spectroscopy of Non-Doped, Hydrogen Terminated CVD Diamond. Physica Status Solidi A, 2000, 181, 77-81.	1.7	5
128	Optical absorption and light scattering in microcrystalline silicon thin films and solar cells. Journal of Applied Physics, 2000, 88, 148-160.	2.5	236
129	Optical properties of microcrystalline materials. Journal of Non-Crystalline Solids, 1998, 227-230, 967-972.	3.1	72
130	Optical determination of the mass density of amorphous and microcrystalline silicon layers with different hydrogen contents. Journal of Non-Crystalline Solids, 1998, 227-230, 876-879.	3.1	65
131	Silicon network relaxation in amorphous hydrogenated silicon. Physical Review B, 1997, 56, R12710-R12713.	3.2	68
132	Enhanced optical absorption in microcrystalline silicon. Journal of Non-Crystalline Solids, 1996, 198-200, 903-906.	3.1	52
133	The Optical Spectra of a-Si:H and a-SiC:H Thin Films Measured by the Absolute Photothermal Deflection Spectroscopy (PDS). Solid State Phenomena, 0, 213, 19-28.	0.3	14
134	Deposition of magnesium silicide nanoparticles by the combination of vacuum evaporation and hydrogen plasma treatment. , 0, , .		2
135	Changes of morphological, optical and electrical properties induced by hydrogen plasma on (0001) ZnO Surface. Physica Status Solidi (A) Applications and Materials Science, 0, , 2100427.	1.8	1